

PAPER • OPEN ACCESS

Optimisation of Sensor Electrode Size for in Electrical Resistance Tomography Implementing Conducting Boundary Strategy

To cite this article: Suzanna Ridzuan Aw *et al* 2021 *J. Phys.: Conf. Ser.* **1874** 012077

View the [article online](#) for updates and enhancements.

A promotional banner for the 240th ECS Meeting. The banner features a colorful striped border at the top. On the left, the ECS logo is displayed in a green circle. To its right, the text reads "240th ECS Meeting" in large blue font, followed by "Oct 10-14, 2021, Orlando, Florida" in a smaller black font. Below this, it says "Register early and save up to 20% on registration costs" in bold black text, and "Early registration deadline Sep 13" in a smaller black font. At the bottom left, there is a red "REGISTER NOW" button. On the right side of the banner, there is a photograph of a diverse group of people in professional attire, smiling and clapping, suggesting a successful event or presentation.

ECS **240th ECS Meeting**
Oct 10-14, 2021, Orlando, Florida
**Register early and save
up to 20% on registration costs**
Early registration deadline Sep 13
REGISTER NOW

Optimisation of Sensor Electrode Size for in Electrical Resistance Tomography Implementing Conducting Boundary Strategy

Suzanna Ridzuan Aw^{1*}, Ruzairi Abdul Rahim², Fazlul Rahman Mohd Yunus², Mohd Hafiz Fazalul Rahiman³, Yasmin Abdul Wahab⁴, Farah Hanan Azimi¹, Lia Safiyah Syafie¹, Nurul Huda Mat Tahir¹, Raja Siti Nur Adiimah Raja Aris¹, Shahrulnizahani Mohammad Din²

¹Faculty of Engineering Technology, University College TATI (UC TATI), Telok Kalong, 24000, Kemaman, Terengganu.

²Process Tomography and Instrumentation Engineering Research Group (PROTOM-i), INFOCOMM Research Alliance, Faculty of Electrical Engineering, Universiti Teknologi Malaysia, 81310 UTM Skudai, Johor, Malaysia.

³Faculty of Electrical Engineering, Universiti Malaysia Perlis, Pauh Putra Campus, 02600 Arau, Perlis, Malaysia.

⁴Department of Instrumentation & Control Engineering (ICE), Faculty of Electrical & Electronics Engineering, Universiti Malaysia Pahang, 26600 Pekan, Pahang, Malaysia.

*Email: suzanna_aw@uctati.edu.my

Abstract. Electrical Resistance Tomography (ERT), due to its diverse advantages has become a promising technique for monitoring and analysing various industrial flows. In this research, an ERT system employing a conducting bubble column was studied because a majority of industrial processes use metal composites for their columns. This paper presents an approach to obtain the optimum size of electrodes in ERT to maximize the capability of an ERT system. A finite element model using COMSOL software was developed to investigate the effect of the electrode size in ERT on sensing field distribution. By adapting the conducting boundary strategies in COMSOL, wider and longer electrodes reduce the potential change near source, suggesting less current density near source. Besides that, wider and longer electrodes also reduce the potential drop and improve the signal strength in Electrical Resistance Tomography. The optimum size of 12 mm x 100 mm electrode is sufficient for the proposed ERT system using conducting bubble column.

1. Introduction

In recent years, the applications of tomographic techniques as a robust non-invasive tool for direct analysis of characteristics of multiphase flows are widely used. One of the applications is to investigate gas holdup distributions in a bubble column which has been the focus of many previous studies [1–10]. Tomography offers a unique opportunity to reveal the complexities of the internal structure of an object without having to invade it. One of the most extensive modalities of tomography is Electrical Resistance Tomography (ERT). ERT is an accepted diagnostic technique for imaging the



interior of opaque systems. It is relatively safe and inexpensive to operate besides being fast, thus enabling real-time monitoring of processes. This technique has been applied in many areas, including medical imaging, environmental monitoring, and industrial processes. There are many researches conducted on ERT. In developing the ERT system, it is vital to consider the sensor selection, which the sensor is the electrode in this research.

The parameters of electrode's characteristic to be considered when adopting ERT are the materials used to construct the sensor, their shape and size, number, and position of the electrodes [11]. In ERT, the electrodes need to be in continuous contact with the fluid inside the vessel which differs from Electrical Capacitance Tomography (ECT). The main medium in contact with ERT sensors has to be conductive to allow injected current to pass through the medium [12]. ECT is used when continuous material such as air or oil does not conduct electricity, whereas for ERT, the continuous material (e.g. water, acids, bases and ionic solutions) is electrically conducting. The voltage measurement in ERT can only be obtained when the injected current finds its conductive pass [13].

This paper investigated and analysed the effect of varying electrode size on the potential distribution of ERT using conducting bubble columns. Modelling and simulation of the system was done by using COMSOL Multiphysics software (simulation software package for various physics and engineering applications).

2. Methodology

Before creating the model using COMSOL, it was decided that a flexible circuit board as the electrode would be used. It is to be noted that metal electrodes for electrically-conducting (metallic) column differ slightly from a non-conducting (insulating) column in which the electrodes need to be insulated from the conducting column. A design was proposed for the electrode fabrication to be implemented in ERT system deploying conducting vessel. Figure 1 and 2 show the design of electrode fabrication using flexible circuit board and an inner cross section view of the proposed system.

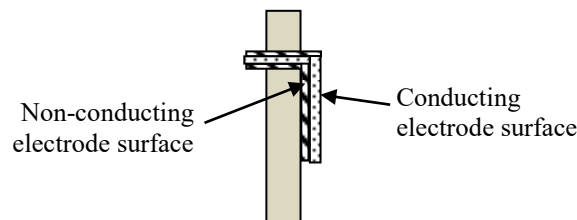


Figure 1. Electrode Fabrication using flexible circuit board

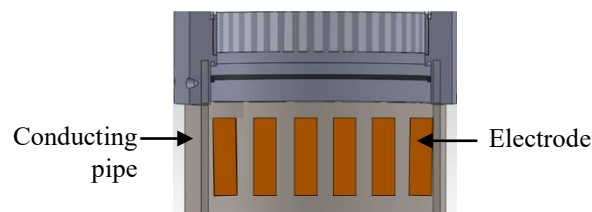


Figure 2. Inner Cross Section View

The number of electrodes selection is a trade-off between the system complexity and image resolution. To address this issue, sixteen rectangular electrodes model were implemented. The electrodes were mounted at the center of the stainless-steel column and evenly spaced along the circumference. As for the injection and measurements, authors employed the same sized electrodes for simplicity of the

upcoming circuit since the loss in measurement sensitivity using larger electrodes is minimal [14]. The parameters used throughout the simulation are shown in Table 1. It is assumed that the electrodes make electrical contact with the fluid inside the column but do not affect the normal mass transfer within the system.

Table 1. Simulation parameters with COMSOL 4.2a

Symbol	Quantity
Column Inner radius	50 mm
Column Outer radius	52.5 mm
Column Height	300 mm
Number of electrodes (N)	16
Electrode's material	Gold
Electrode's height (h)	10 mm, 20 mm,..., 110 mm, 120mm
Electrode's width (w)	3mm, 6 mm, ..., 15 mm, 18 mm
Current excitation	20 mA
σ_{water}	5×10^{-3} S/m

Prior to building a model using COMSOL Multiphysics, users need to specify the desired space dimension, select physics interfaces and study type. A 3D space dimension, *Electric Currents* of physics interface under the *AC/DC* branch and stationary study were selected respectively for the simulation study. After that, the following steps were taken:

i. Create a physical model using available geometries:

A 3D physical model has been developed such that it mimics a real system. Sixteen electrodes that were insulated from the column wall were placed equidistantly inside the column.

ii. Define materials for each domain in the created model:

The materials for each related domain in the model were defined such that it also resembles a real one. The column itself was defined as stainless steel material and the main medium inside the column was the water with a conductivity of 5 mS/m.

iii. Assign relevant physics interface and define boundary and initial conditions that describe real experiment setup:

Electric Currents interface was chosen since it would produce an electrical field and has the electrical potential distribution required for the analysis. It also contained the equations, boundary conditions, and current sources for modelling electric currents in conductive media, solving the electric potential. By adopting the conducting boundary strategy, a constant current of 20 mA was applied at source electrode, e_s and the output voltages from 15 pairs of electrodes from e_1 to e_{15} were measured. Meanwhile, the column itself was grounded and acted as the current sink. The cross-section view of the 3D COMSOL Multiphysics model is in Figure 3.

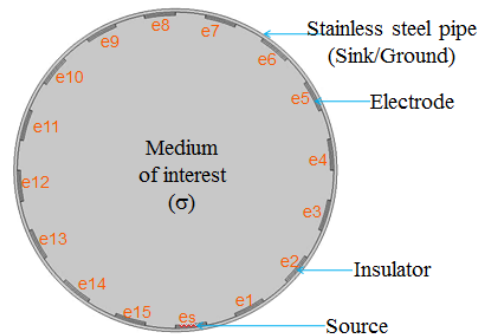


Figure 3. Cross Section View of 3D COMSOL Model

iv. Mesh the model

In a simulation process, meshing geometry can be crucial in obtaining the best results in faster way. Extra fine meshing under meshing physics-controlled setting is chosen since denser meshing would provide a more reliable finite element method (FEM) simulation. Figure 4 shows the meshed system under investigation.

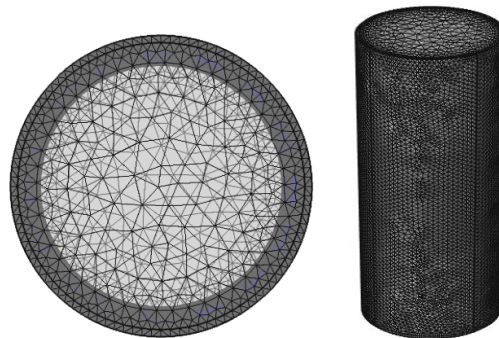


Figure 4. Extra Fine Meshing using COMSOL

v. Run the study:

The investigated model is simulated using the default solver under stationary study. In applying the stationary solver, it is assumed that the load and deformation do not vary in time. All modelling formulations are based on Maxwell's equation. The physic interface chosen earlier solves the current conservation equation for the electric potential.

To solve for varying length and width, a *Parametric Sweep* study node has been added to the study to perform parametric variation. *Parametric Sweep* study find a solution to a sequence of PDE problems that arise the parameters of interest are varied. The parameters which are the electrode length and width in this case are globally defined in the model.

vi. Pre-process the data for result analysis

Last but not least, the results are pre-processed and analysed and were presented in the next section.

3. Results and Discussion

The simulation results of the ERT model using stainless steel pipe are presented in this section. In this study, the potential distributions produced by varying the size of the electrodes of a 20 mA current source were analysed. Firstly, the effects of varying electrode height, h for different electrode width, w

(5 mm, 10 mm, 12 mm) in a homogeneous solution were analysed. These are shown in Figure 5, 6 and 7. The potential profiles at each electrode excluding the source were plotted in Figure 5a, 6a and 7a correspondingly. As can be seen from Figure 5a, 6a, and 7a, different electrode heights produced different output values and the values are significantly larger for the electrodes near to the source. The output potential was significantly higher near the current injection electrodes and slightly smaller for the longer electrodes at other locations. For different electrode heights, electric potential at the nearest and furthest electrodes from source were observed in Figure 5b, 6b and 7b. From the simulations, it is found that the electric potential for e_1 of 10 mm length is smaller than 20 mm length. According to the literature that had been done, it is believed that this is due to the equipotential averaging and electrode size trade off as been discussed in [14]. Ideally, a small surface area preferably a needle point is desired for voltage measurement. This is to avoid averaging several equipotential at that particular electrode. So, it is believed that, for 10 mm electrode length of e_1 , it did average several equipotential which made the output smaller than 20 mm length. As the length is increased, more equipotential were being averaged at the electrode surface.

Starting from 20 mm length till 120 mm, it is noticed that the potentials difference between e_1 and e_8 slowly decreasing as the electrodes get longer. Electrodes with greater length reduced the potential near the excitation which is the result of less current density near the excitation electrode. In addition to that, based on Ohm's Law and resistance equation, it is found that the output potential is inversely proportional with the surface area of the electrode in which the surface area includes the length and width of the electrode. When varying the electrode's height for different electrode's width, it is observed that the output potential reading especially the one near to the source electrode becomes higher as the width is increased. The effect of increasing the width is discussed thoroughly latter.

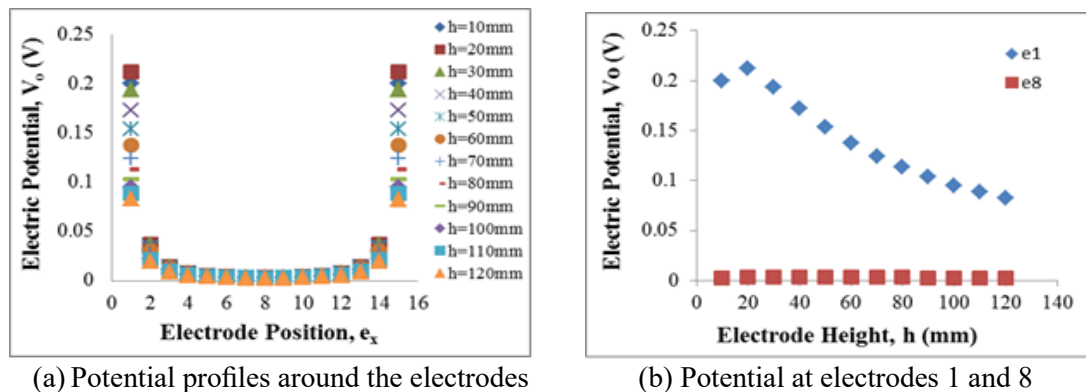


Figure 5. Effect of Varying Electrode Height for 5 mm Electrode Width

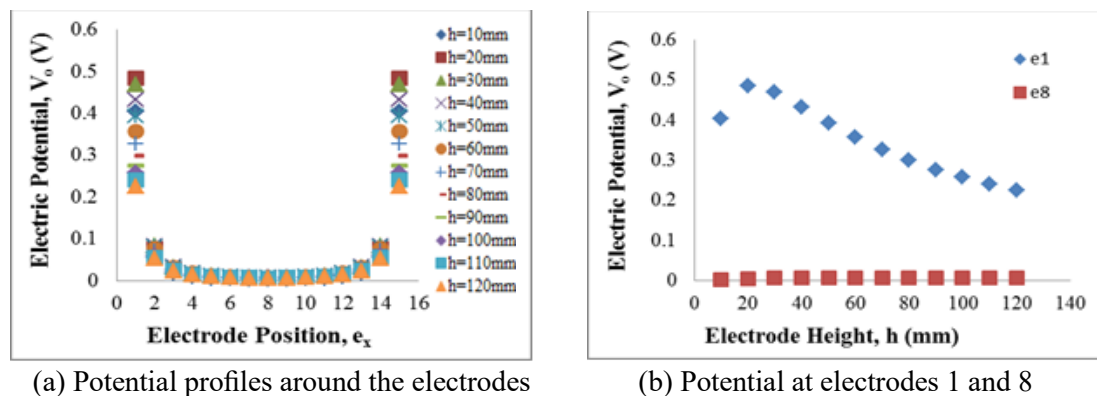


Figure 6. Effect of Varying Electrode Height for 10 mm Electrode Width

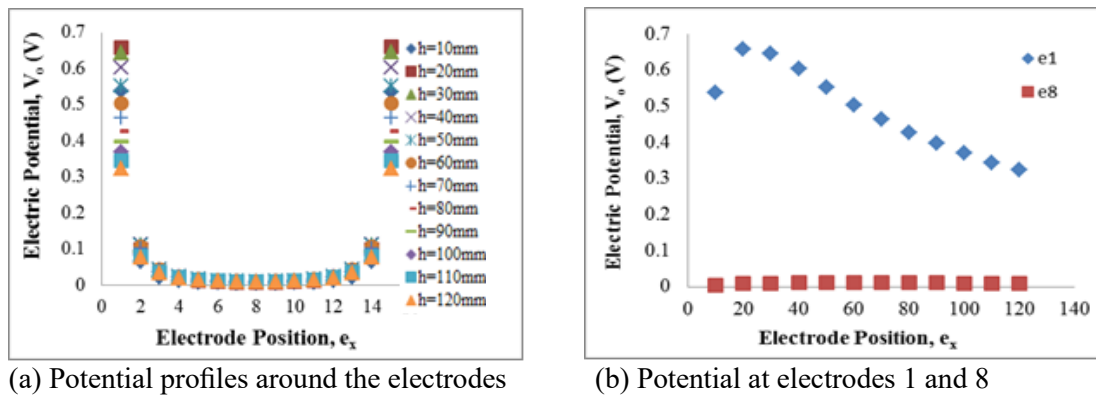


Figure 7. Effect of Varying Electrode Height for 12 mm Electrode Width

Electrodes with greater axial length would slower the attenuation of the sensing field around the centre plane where the electrode’s centre is located. In addition, the sensing field would have better uniformity and space distribution of the sensing field was expanded [15]. Increasing the electrode height would improve the evenness of the sensing field as shown in Figure 8. The potential distributions in the figure obtained from COMSOL are for the electrodes with height of 30 mm, 60 mm and 100 mm.

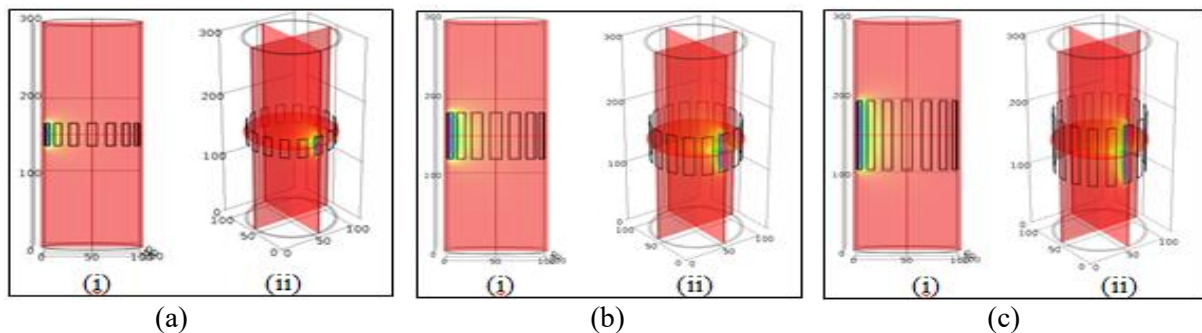
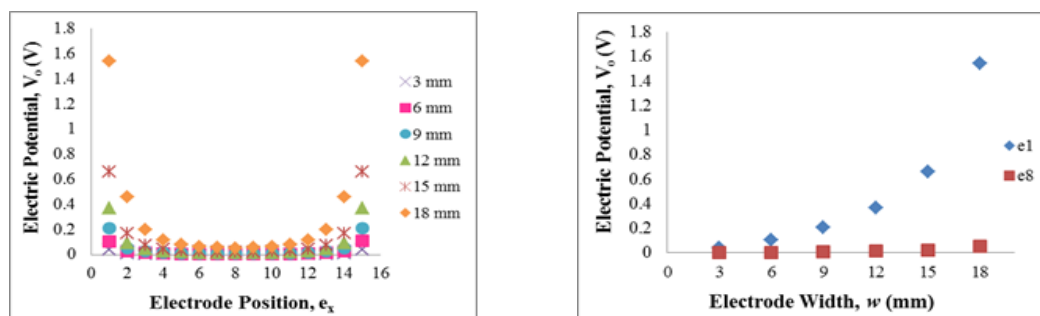


Figure 8. Potential Distribution in COMSOL for Different Electrode Heights

(i) yz-plane view (ii) 3D view
 (a) h = 30 mm, (b) h = 60 mm, (c) h = 100 mm

By choosing an electrode height that equals 100 mm, the effects of varying electrode width, w of 3 mm, 6 mm, 9 mm, 12 mm and 18 mm on potential distribution were simulated and analysed. Figure 9a shows the potential distribution for the homogeneous systems of each width mentioned earlier. Meanwhile, Figure 9b shows the potential between the nearest and furthest electrode from the source, e_s .



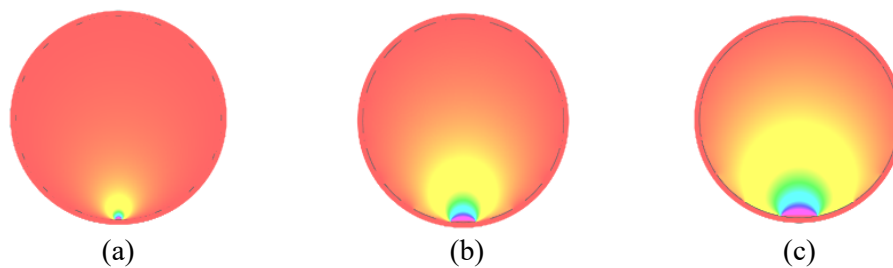
(a) Potential profile around the electrodes

(b) Potential at electrodes 1 and 8

Figure 9. Electric Potential Distribution of Varying Electrode Width

As can be seen, the electric potential of the electrodes especially the one near to the source produce higher output as the width increased. In addition to that, the potential difference for the electrode nearest, e1 and furthest, e8 from the source also becomes greater when the width is wider. This is due to the higher current densities of the wider electrodes. From the results in Figure 9, it is concluded that wider electrodes improve the signal strength of the system which will also improve the ability of object detection.

To illustrate the potential distributions for different electrode widths obtained in COMSOL Multiphysics, the xy-plane of the results are presented in Figure 10. Wider electrodes provide a more uniform current distribution in the region of interest. In addition to that, it improves the evenness of the field distribution resulting in improved signal strength. However, narrower electrodes must be used when a higher number of electrodes are placed around the circumference to avoid shunting where the current bypasses the medium and goes around the circumference [16].

**Figure 10.** Potential Distribution Obtained using COMSOL for Different Electrode Widths(a) $w = 3$ mm, (b) $w = 12$ mm, (c) $w = 18$ mm

The sensitivity of the electrode width on anomaly detection was examined further using a spherical inclusion (inclusion diameter $D=10$ mm). The inclusion is the phantom of bubble. A sensor sensitivity indicates how much the sensor output changes when the measured quantity changes. Sensors that measure very small changes must have very high sensitivity. Figure 11 shows the potential change $\Delta V/V_h$ with respect to the corresponding potential measured in the homogenous medium induced by the spherical inclusion. The positive potential differences for electrodes near to the source (e1, e2, e3, e13, e14 and e15) were in response of the higher current densities near source electrode, e_s . The potential difference corresponding to the homogeneous medium drops to a negative value for e_4 to e_{12} as the current densities deteriorate as it travels through the medium. Overall, the responses became more sensitive when the electrode width is bigger and it was observed that 12 mm electrode width is the most sensitive towards the inclusion. The sensitivity became lower for electrode width of 15 mm and above possibly due to the shunting effect mentioned earlier.

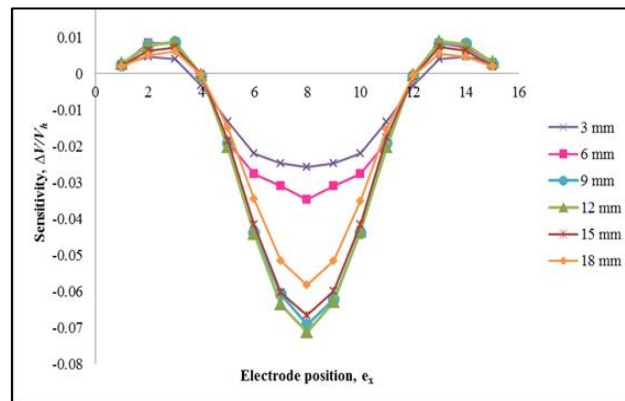


Figure 11. Sensitivity of The Electrode Width on Anomaly Detection of a Spherical Inclusion

4. Conclusion

An electrode size needs to be identified before setting up the final hardware of an ERT system. Ideally, the injection electrode should be as large as possible while the measuring electrodes should be as small as possible. The size related trade-off has to be considered since the electrodes are alternately used for injection and measurement electrodes. It is suggested that electrode size of 12 mm x 100 mm is good and sufficient for the ERT system using metal wall. Results from the simulation clearly show that wider and longer electrodes reduce the potential change near source, suggesting less current density near source. Besides that, wider and longer electrodes also reduce the potential drop and improve the signal strength in ERT. The numerical method has proven that the optimum electrode width should cover 60% of the sensing surface and electrodes with greater height produce better axial field distribution. Normally, improving the evenness of the current distribution always counteract the shunting effect of the system. By taking into account the effects of varying electrode sizes, the electrode width must be carefully selected to prevent the shunting effects in ERT. Last but not least, it is to be state that the electrode size of 12 mm x 100 mm has been applied to the conducting bubble column successfully in the experiment.

5. References

- [1] Singh BK, Quiyoom A, Buwa V V. 2017 Dynamics of gas–liquid flow in a cylindrical bubble column: Comparison of electrical resistance tomography and voidage probe measurements. *Chem Eng Sci* **158** 124–139.
- [2] Hernandez-Alvarado F, Kleinbart S, Kalaga D V., et al. 2018 Comparison of void fraction measurements using different techniques in two-phase flow bubble column reactors. *Int J Multiph Flow* **102** 119–129.
- [3] Vadlakonda B, Mangadoddy N. 2017 Hydrodynamic study of two phase flow of column flotation using electrical resistance tomography and pressure probe techniques. *Sep Purif Techno*; **184** 168–187.
- [4] Jin H, Lian Y, Qin Y, et al. 2013 Distribution characteristics of holdups in a multi-stage bubble column using electrical resistance tomography. In: *Particuology*. **11(2)** 225–23.
- [5] Jin H, Wang M, Williams RA. 2007 Analysis of bubble behaviors in bubble columns using electrical resistance tomography. *Chem Eng J* **130** 179–185.
- [6] Sardeshpande M V., Gupta S, Ranade V V. 2017 Electrical resistance tomography for gas holdup in a gas-liquid stirred tank reactor. *Chem Eng Sci* **170** 476–490.
- [7] Ridzuan Aw S, Abdul Rahim R, Fazalul Rahiman MH, et al. 2015 Simulation study on electrical resistance tomography using metal wall for bubble detection. *J Teknol* **73** 31–35.
- [8] Babaei R, Bonakdarpour B, Ein-Mozaffari F. 2015 The use of electrical resistance tomography for the characterization of gas holdup inside a bubble column bioreactor containing activated sludge. *Chem Eng J* **268** 260–269.

- [9] Adegoke TB, Wang M. 2012 Gas hold-up analysis of a highly viscous ionic liquid in a bubble column using electrical resistance tomography. In: *6th International Symposium on Process Tomography*..
- [10] Adetunji O, Rawatlal R. 2017 Estimation of bubble column hydrodynamics: Image-based measurement method. *Flow Meas Instrum* **53** 4–17.
- [11] Aw SR, Rahim RA, Rahiman MHF, et al. 2014 Electrical resistance tomography: A review of the application of conducting vessel walls. *Powder Technology* **254** 256–264.
- [12] Sharifi M, Young B. 2013 Electrical resistance tomography (ert) applications to chemical engineering. *Chemical Engineering Research and Design* **91**1625-1645.
- [13] Gu J, Yin W, Wang C, et al. 2009 Modeling of the conductive ring electrical impedance tomography sensor. In: *ICEMI 2009 - Proceedings of 9th International Conference on Electronic Measurement and Instruments*.
- [14] Dickin F, Wang M. 1996 Electrical resistance tomography for process applications. *Meas Sci Technol* **7(3)** 247–260.
- [15] Ma Y, Wang H, Xu LA, et al. 1997 Simulation study of the electrode array used in an ERT system. *Chem Eng Sci* **52(13)** 2197–2203.
- [16] Lee JY, Santamarina JC. 2010 Electrical resistivity tomography in cylindrical cells-guidelines for hardware pre-design. *Geotech Test J* **33(1)**

Acknowledgement

The authors fully acknowledged University College TATI for the approved fund which makes this important research viable and effective. Also, special thanks to PROTOM research group from Universiti Teknologi Malaysia for their honourable support and cooperation.